16th World Conference on Earthquake, 16WCEE 2017

Santiago Chile, January 9th to 13th 2017

Paper N° 804 (Abstract ID)

Registration Code: S-B1460358481

Seismic Behavior of R/C Beam Using High Strength Longitudinal Rebars

Yoshiaki Ikenuma[(1)], Makoto Maruta [(2)], Satoru Nagai [(3)]

[(1)] *Japan , Tokyo Tekko Co.,Ltd. , yoshiaki_ikenuma@tokyotekko.co.jp*
[(2)] *Japan , Shizuoka Institute of Science and Technology , maruta@riko.shimane-u.ac.jp*
[(3)] *Japan , SK Service Co.,Ltd., snagai@sk-svc.com*

Abstract

Recently, many high-rise Reinforced Concrete buildings are built using high strength materials in Japan.

The combination of high strength concrete and high strength rebars is a good match for seismic members.

However, middle rise reinforced concrete buildings are constructed using concrete with strength in the range of 21 to 60N/mm^2, and rebars with yield strength between 350 and 500N/mm^2.

To conduct research to use combined high strength rebars and normal strength concrete, it is important to rationalize reinforcing bar work on middle rise reinforced concrete buildings.

But few experiments have been conducted to confirm the seismic behavior obtained by combining rebars with yield strength of about 600N/mm^2 and concrete with strength between 21 and 60N/mm^2.

Therefore, a total of 13 beam specimens were tested to evaluate the seismic capacities and the design method. The specimens are 1/2 scaled beams.

The beams were subjected to anti-symmetrical reversal loads as seismic motion of a frame structure.

As common parameters, the section shape was 300mm*400mm at 1/2 scale and the shear span ratio was 2.5, and the main bars used were rebars with yield strength ranging from 628 to 640N/mm^2.

The failure mode of the beam members was varied and planned for concrete strength from 21 to 60N/mm^2.

The actual strength of the concrete was 22.5N/mm^2 for Fc21, 38.7N/mm^2 for Fc36, and 64.9N/mm^2 for Fc60.

The test confirmed the load-bearing capacity during bending failure, shear failure and bond-splitting failure.

This experiment also revealed that the load-bearing capacity equations induced by many past research projects are effective.

The strength equations of several failure are verified by this test and by past studies.

The skeleton curve for seismic design using these testing data is proposed.

The skeleton curve is composed of initial stiffness, a degrading ratio after cracking and yield strength. The degrading ratio for beams using high strength longitudinal rebars is newly proposed by this paper.

Not only a test, but also an analytical study was carried out to grasp the detailed behavior of beams.

The design method including its criteria and structural capacity can be proposed for use for design of low or middle rise R/C buildings in an earthquake-prone country.

Keywords: R/C Beam , Bar of 600N/mm^2 yield strength , Degrading ratio for beams

1. Introduction

In recent years, many high-rise RC buildings of 30 or more stories have been constructed in Japan using high strength concrete and high strength rebars.

Medium-rise RC buildings from 15 to 20 stories on the other hand, are often constructed using concrete with concrete strength between 21 and 60N/mm^2 and rebars with yield strength from 350 to 500N/mm^2.

It is important to study combining and using high strength rebars and normal strength concrete in order to rationalize the rebar work of medium-rise RC buildings. But few tests have confirmed the seismic behavior of members made by combining rebars with yield strength of 600N/mm^2 and concrete with strength from 21 to 60N/mm^2.

To confirm the seismic behavior of and establish a design method for this combination, a total of thirteen 1/2-scale beam members were tested.

2. Specimen

Table 1 shows the list of specimens. Fig. 1 shows an example of a bar arrangement drawing and Fig. 2 shows the cross-section of a specimen.

The specimens were a total of thirteen 1/2-scale beam and assumed three forms of failure, bending failure, bond splitting failure and shear failure. The specimen section (b×D) was basically 300mm× 400mm, and B8, B9 specimens in the bonding splitting failure form was 240mm×400mm. All factors were harmonized to set the forms of failure. The shear span to depth ratio (M/QD) was two standards of 2.0 and 2.5.

The longitudinal rebars were of two standards: SD400 rebars and SD600 rebars. SD600 presents the yield strength of at least 600N/mm^2. The concrete design strength (Fc) was 3 standards: 21, 36, and 60N/mm^2. The tensional rebar ratio (pt) was 6 standards: 0.96, 0.99, 1.29, 1.32, 1.94, and 2.39%. The shear rebars were of 2 standards: SD295 rebar and SD785 rebar. The shear rebar ratio (pw) was set at 5 standards: 0.21, 0.42, 0.68, 0.84, and 1.19%.

Table 1 – List of specimens

<table>
<tr><th rowspan="2">Name</th><th rowspan="2">B×D
(mm)</th><th rowspan="2">Internal span L
(mm)</th><th rowspan="2">Shear span ratio
M/QD</th><th rowspan="2">Fc</th><th colspan="5">Longitudinal rebar</th><th colspan="6">Shear rebar</th><th rowspan="2">Design failure form</th></tr>
<tr><th>Number of tensional rebars</th><th>Rebar diameter</th><th>pt
(%)</th><th>Steel grade</th><th>pt・σy
(N/mm^2)</th><th>Rebars</th><th>Rebar diameter</th><th>Interval
(mm)</th><th>pw
(%)</th><th>Steel grade</th><th>pw・σwy</th></tr>
<tr><td>P1</td><td rowspan="11">300×400</td><td rowspan="4">1600</td><td rowspan="4">2.0</td><td rowspan="4">36</td><td>4</td><td rowspan="4">D22</td><td>1.29</td><td>SD600</td><td>7.74</td><td rowspan="11">4</td><td rowspan="4">D10</td><td rowspan="2">80</td><td rowspan="2">1.19</td><td rowspan="4">SD295</td><td rowspan="2">3.51</td><td>F or FB</td></tr>
<tr><td>P2</td><td>6</td><td>1.94</td><td rowspan="2">SD400</td><td>7.74</td><td>F</td></tr>
<tr><td>P3</td><td rowspan="2">4</td><td rowspan="2">1.29</td><td>5.16</td><td rowspan="2">140</td><td rowspan="2">0.68</td><td rowspan="2">2.00</td><td>FS</td></tr>
<tr><td>P4</td><td rowspan="10">SD600</td><td>7.74</td><td>B or FSB</td></tr>
<tr><td>B1</td><td rowspan="9">2000</td><td rowspan="9">2.5</td><td>21</td><td rowspan="4">4</td><td rowspan="4">D19</td><td rowspan="4">0.96</td><td rowspan="4">5.73</td><td rowspan="9">D6</td><td>50</td><td>0.84</td><td rowspan="4">SD785</td><td>6.63</td><td>F</td></tr>
<tr><td>B2</td><td>36</td><td>100</td><td>0.42</td><td>3.31</td><td>F</td></tr>
<tr><td>B3</td><td>60</td><td>150</td><td>0.28</td><td>2.21</td><td>F</td></tr>
<tr><td>B4</td><td rowspan="3">21</td><td rowspan="2">200</td><td rowspan="2">0.21</td><td>1.66</td><td>FB or B</td></tr>
<tr><td>B5</td><td>8</td><td rowspan="3">D16</td><td>1.32</td><td>7.94</td><td>SD295</td><td>0.62</td><td>FS or S</td></tr>
<tr><td>B6</td><td rowspan="2">6</td><td rowspan="2">0.99</td><td rowspan="2">5.96</td><td>50</td><td>0.84</td><td rowspan="4">SD785</td><td>6.63</td><td>F</td></tr>
<tr><td>B7</td><td>36</td><td>100</td><td>0.42</td><td>3.31</td><td>F</td></tr>
<tr><td>B8</td><td rowspan="2">240×400</td><td rowspan="2">21</td><td rowspan="2">8</td><td rowspan="2">D19</td><td rowspan="2">2.39</td><td rowspan="2">14.33</td><td>2</td><td>125</td><td>0.21</td><td>1.66</td><td>B</td></tr>
<tr><td>B9</td><td>4</td><td>125</td><td>0.42</td><td>3.31</td><td>B</td></tr>
</table>

Failure forms: F is bending failure; B is bond splitting failure; S is shear failure, FB is bond splitting failure after bending failure, and FS is shear failure after bending failure.

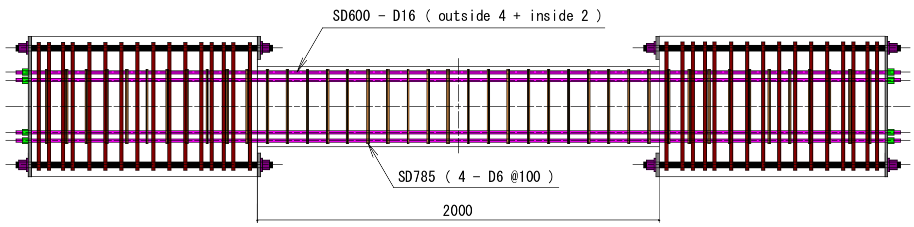

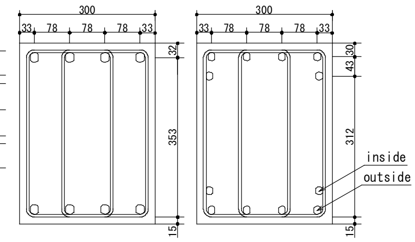

Fig.1 – Rebar arrangement of specimen (B7) Fig.2 – Cross-section of specimen

The P1 specimen was made by arranging four SD600-D22 (D: Diameter) tension rebars in one layer (outside; in Fig.2), and the P2 specimen by arranging six SD400-D22 tension rebars in two layers (outside and inside; in Fig.2). In order for the maximum strengths to generally conform, the steel grade and number of the tensional rebars were varied.

B1 and B2 specimens made by arranging four D19 tension rebars in one level and B6 and B7 specimens were made by arranging six D16 tensional rebars in two layers, which are called the outside and the inside. The (pt) was caused to generally conform by varying the rebars' diameters.

3. Material Properties

Table 2, Table 3 shows the mechanical characteristics of the rebars and concrete, respectively. The compressive strength of the concrete generally corresponded with the planning strength at all 3 standards.

The yield strength of the longitudinal rebars was 430 N/mm^2 for SD400 and from 627 to 642 N/mm^2 for the SD600.

The yield strength of the shear rebars was from 366 to 414 N/mm^2 for the SD295 and 924 N/mm^2 for the SD785.

Table 2 – Mechanical characteristics of rebar

Type	Yield point or 0.2% bearing capacity (N/mm^2)	Tensile strength (N/mm^2)	Young's modulus (×10^{5}N/mm^2)	Yield strain or strain at 0.2% bearing capacity (μ)
SD400-D22	430	578	1.92	2437
SD600-D16	632	766	1.93	3407
SD600-D19	642	808	1.91	4007
SD600-D22	627	788	1.94	3620
SD295-D6	414	535	1.84	4286
SD295-D10	366	507	1.97	1962
SD785-D6	924	1081	1.84	7036

Values are average values of tensile test results of 3 specimens

Fig. 3 shows the stress – strain curve of the SD600-D16 rebars. Its rebars clearly have yield points and yield shelves.

4. Test Method

Fig. 4 is an outline of the loading equipment. Photo 1 shows circumstances during testing.

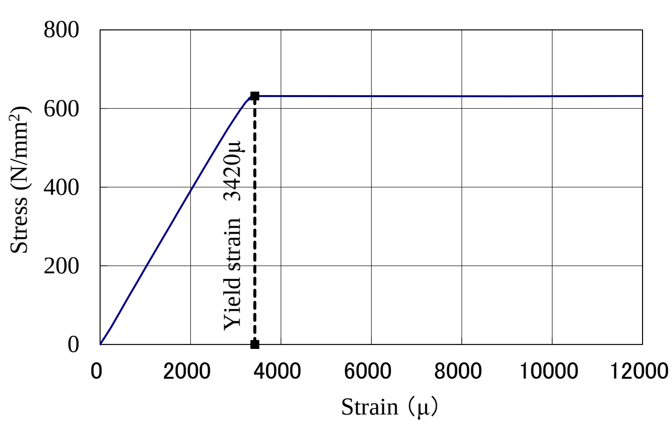

Fig. 3 – stress –strain curve of the SD600-D16 rebar

Table 3 – Mechanical characteristics of concrete

Fc	Max. dimension of coarse aggregate (mm)	Name	Compressive strength (N/mm^2)	Young's modulus (×10^{4}N/mm^2)	Poisson's ratio
21	13	B1	22.5	2.55	0.146
		B4	22.1	2.58	0.164
		B5	22.1	2.52	0.140
		B6	22.1	2.58	0.124
		B8	22.3	2.56	0.151
		B9	21.3	2.68	0.153
36		P1	39.2	2.86	0.181
		P2	39.0	2.81	0.166
		P3	38.3	2.83	0.178
		P4	39.5	2.88	0.190
		B2	38.7	2.99	0.164
		B7	38.7	2.99	0.164
60		B3	64.9	3.54	0.185

Reversal loading was R=1.25 x 10^{-3}rad once under displacement control at deformation angle R to cause anti-symmetric moment in the beam, and reversal loadings twice at 2.5, 5.0, 10, 15, 20, and 40 x 10^{-3}rad (Fig.5).

Fig. 6 shows the locations of displacement transducers that measure the relative displacement. Total deformation (δ) was measured as the average value of the relative displacement obtained by installing displacement gauges (DC1 and DC2) on measurement jigs protruding from stubs on the left and right.

The deformation angle (R) was a value obtained by dividing the total deformation (δ) by the length of the internal span of the beam (L0).

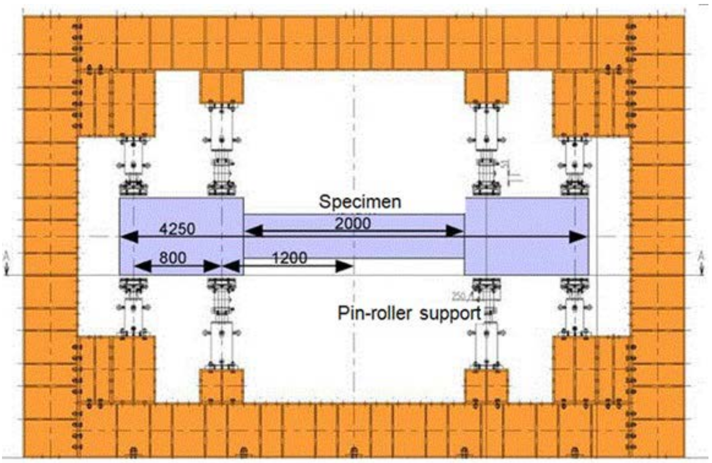

Fig.4 – Loading equipment

5. Test Results

5.1 Damage Transition

Bending cracks of all specimens occurred at R = +1.25 x 10^{-3}rad. In only B3 of Fc60, bending cracks occurred at R = +2.5 x 10^{-3}rad.

Shear cracks occurred in all specimens at R = +2.5 ～ +5.0 x 10^{-3}rad. Later, in P1 to P3, B1 to B3, B6 and B7 specimens, in which bending failure occurred, the longitudinal rebars yielded at R = +15 x 10^{-3}rad. In B4, B8, and B9 specimens, in which bond splitting failure occurred, yielding was not reached in any longitudinal rebars and shear rebars up to maximum strength.

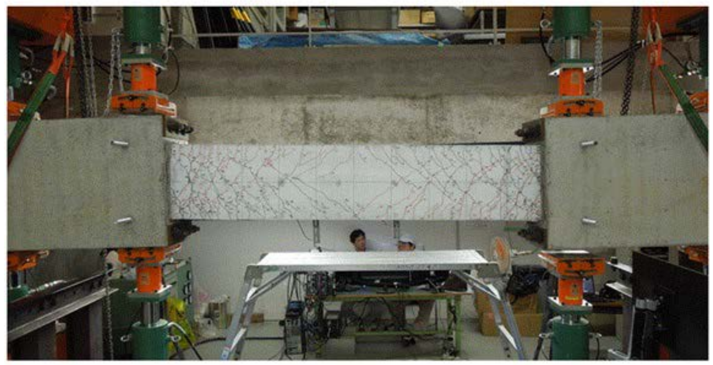
Photo 1 – Under testing

In P4 specimens, the planned bending failure did not occur, and the shear rebars yielded at R = +15 x 10^{-3}rad. In B5 specimen, in which shear failure occurred, the shear rebars yielded at R = +15 x 10^{-3}rad.

Table 4 shows photos of cracking behavior of specimens at R = +5.0 and +40.0 x 10^{-3}rad.

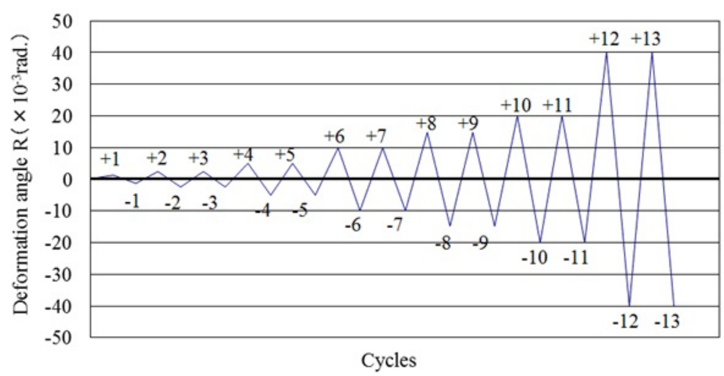

Fig. 5 – Loading plan

When the P1 specimen with SD600-D22 arranged in only the outside and the P2 specimen with SD400-D22 arranged in the outside and the inside, which were planned so their bending ultimate strengths would be equal, were compared, when R = +5.0 x 10^{-3}rad , P2 specimen with its inside longitudinal rebar showed more cracks in the center of the specimen. But at R = +40.0 x 10^{-3}rad , the P1 specimen showed far wider cracks.

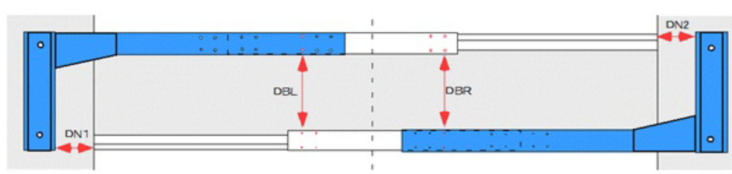

Fig. 6 – Displacement transducers

When the B1 specimen with four SD600-D19 arranged in only the outside and B6 specimen with six SD600-D16 arranged in the outside and the inside, which were planned so that their bending ultimate strengths would be equal, were compared, when R = +5.0 x 10^{-3}rad , B6 specimen with its inside longitudinal rebars shows more cracks in the center of the specimen. At R = +40.0 x 10^{-3}rad , B1 and B6 specimens had cracks of about the same width.

Table 4 – Cracking behavior

Deformation angle	P1	P2	P3
+5.0 ($\times 10^{-3}$rad.)	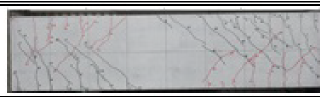	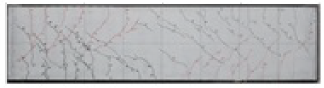	
+40.0 ($\times 10^{-3}$rad.)			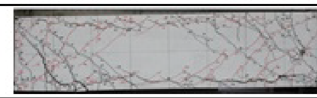
Deformation angle	P4	B1	B2
+5.0 ($\times 10^{-3}$rad.)	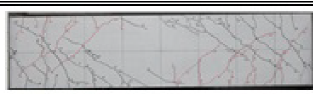		
+40.0 ($\times 10^{-3}$rad.)	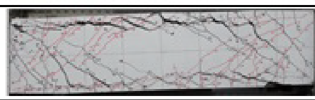		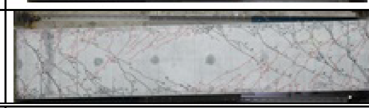
Deformation angle	B3	B4	B5
+5.0 ($\times 10^{-3}$rad.)			
+40.0 ($\times 10^{-3}$rad.)		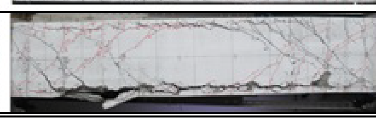	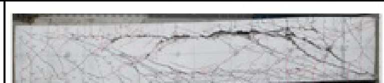
Deformation angle	B6	B7	B8
+5.0 ($\times 10^{-3}$rad.)			
+40.0 ($\times 10^{-3}$rad.)			
Deformation angle	B9		
+5.0 ($\times 10^{-3}$rad.)	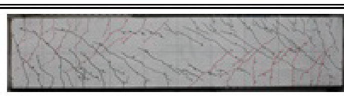		
+40.0 ($\times 10^{-3}$rad.)			

5.2 Response

Fig. 7 shows the shear force (Q) – deformation angle (R) relationship for all the specimens.

The P1 specimen using SD600 recorded maximum strength of 414.8kN. Later, the strength failed to rise as the deformation angle approached its peak of R = +40 x 10^{-3}rad , and it fell below 80% of the maximum strength. The bond stress distribution confirmed that the longitudinal rebars had slipped.

In the P2 specimen, which used SD400 and had almost the same bending ultimate strength as the P1 specimen, yield of both outside and inside rebars was confirmed at R=15 x 10^{-3}rad. Later, maximum strength of 437.0 kN was recorded on the R = +40 x 10^{-3}rad positive side. The P2 specimen was stiffer than the P1 specimen.

In the P3 specimen, which used SD400 and the consistent P1 specimen with (pt), the rebars yielded at the peak of R = -10 x 10^{-3}rad , and maximum strength of 296.6 kN was recorded at R = +15 x 10^{-3}rad. Later at R = +40 x 10^{-3}rad it was lower than 80% of maximum strength.

In the P4 specimen, which was the smaller (pw) than the P1 specimen, shear rebars yielded at R = +15 x 10^{-3}rad , and maximum strength of 396.9 kN was recorded. It fell below 80% of the maximum strength at R = +20 x 10^{-3}rad.

In the B1 specimen of Fc21, B2 specimen of Fc36, and B3 specimen of Fc60, with smaller diameter longitudinal rebars than in the P1 specimen, to increase the bond capacity, the rebars yielded at the peak of R = +15 x 10^{-3}rad. In the B1-B3 specimens, the maximum strength was recorded at the peak of R = +40 x 10^{-3}rad. This result confirmed that it is possible to prevent bond splitting failure.

B4 is a specimen with only the outside longitudinal rebars planned to confirm the behaviour of bonding of SD600 and Fc21 concrete. It recorded maximum strength of 224.6 kN at R = +15 x 10^{-3}rad. Neither its longitudinal rebars nor shear rebars yielded, cracks that are bond splitting opened at R = +20 x 10^{-3}rad , and fell below 80% of the maximum strength.

The B5 specimen was planned to confirm the shear properties of SD600 and Fc21 concrete. Shear cracks opened abruptly at R = +15 x 10^{-3}rad. Its maximum strength was 229.6 kN. Loading was done up to R = +40 x 10^{-3}rad , without any abrupt decline of strength. This confirmed the usability of SD600.

B6 and B7 are specimens with outside and inside longitudinal rebars according with the bending ultimate strength of the B1 and B2 specimens respectively. The B1 and B2 specimens similarly confirmed yielding of the outside longitudinal rebars at R = +15 x 10^{-3}rad. The maximum strength was recoded at R = +40 x 10^{-3}rad , confirming equal deformation capacity of the B1 and B2 specimens.

The B8 specimen was planned to confirm bond slipping failure prior to rebar yielding, with longitudinal rebars arranged in the outside and the inside and shear rebars only in the outer peripheral without sub-ties. Maximum strength of 223.2 kN was recoded at R = +15 x 10^{-3}rad , but the calculated bond value of 273.0 kN was not reached. It was revealed that in this specimen without sub-ties it is difficult to apply the bond splitting equation Ref. [4].

The B9 specimen is planned to confirm bond slipping failure prior to rebar yielding, and the shear rebars were added as the sub-ties towards the B8 specimen. Maximum strength of 344.7 kN was recorded at R = +15 x 10^{-3}rad , and the calculated bond value of 313.2 kN was exceeded.

This result revealed that in a case where SD600 is used, it is necessary to insert sub-ties in order to prevent early bond splitting failure.

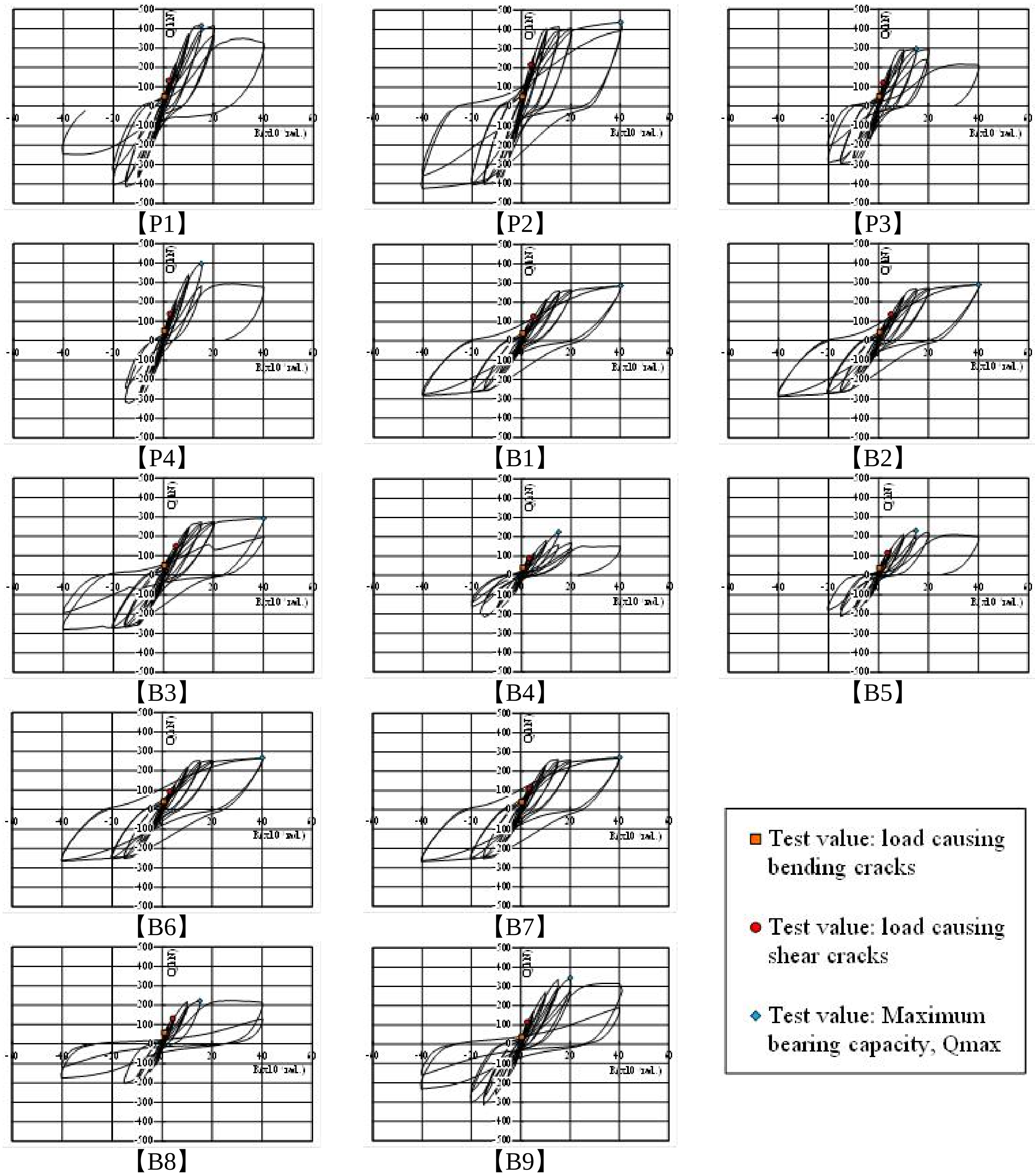

Fig. 7. – Shear force Q and deformation angle R relationship

6. Discussion of ultimate strength

6.1 Results of calculation by the equations

Table 5 shows the strength calculation results based on the equations and test results. The bending ultimate strength was obtained by the equations of Ref. [1] and [2]. The shear ultimate strength used the equation of Ref. [3] and the bond splitting strength used the equation of Ref. [4].

In this chapter, each strength comparison between these test results and the calculations of current proposed equations, are discussed.

Table 5 – The relationship of the maximum strength with the calculated value of the equations

Name	Calculated values												Test results	
	Bending ultimate strength (Ref.1 Eq.) Q_{fu1} (kN)	$\frac{Q_e}{Q_{fu1}}$	Bending ultimate strength (Ref.2 Eq.) Q_{fu2} (kN)	$\frac{Q_e}{Q_{fu2}}$	Shear ultimate strength (Ref.3 Eq.) (Rp=0) Q_{su0} (kN)	$\frac{Q_e}{Q_{su0}}$	Shear ultimate strength (Ref.3 Eq.) (Rp=0.02) Q_{su2} (kN)	$\frac{Q_e}{Q_{su2}}$	Bond splitting strength (Ref.4 Eq.) (Rp=0) Q_{bu0} (kN)	$\frac{Q_e}{Q_{bu0}}$	Bond splitting strength (Ref.4 Eq.) (Rp=0.02) Q_{bu2} (kN)	$\frac{Q_e}{Q_{bu2}}$	Maximum strength Q_e (kN)	Failure form
P1	394.3	1.05	400.7	1.04	787.9	0.53	420.3	0.99	614.1	0.68	398.8	1.04	414.8	FB
P2	385.0	1.14	393.7	1.11	786.2	0.56	420.3	1.04	743.6	0.59	397.5	1.10	437.0	F
P3	270.4	1.10	278.4	1.07	531.4	0.56	248.3	1.19	459.0	0.65	313.6	0.95	296.6	FS
P4	394.3	1.01	400.8	0.99	534.4	0.74	250.4	1.58	464.2	0.86	315.8	1.26	396.9	B
B1	239.7	1.19	240.3	1.19	686.8	0.42	481.7	0.59	436.8	0.66	307.5	0.93	286.3	F
B2	239.7	1.20	245.1	1.18	711.8	0.41	355.0	0.81	363.7	0.79	268.9	1.07	288.7	F
B3	239.7	1.22	250.1	1.17	556.0	0.53	272.9	1.08	405.3	0.72	293.2	1.00	293.4	FS
B4	239.7	0.94	240.2	0.94	357.1	0.63	170.8	1.31	245.0	0.92	179.2	1.25	224.6	B
B5	302.3	0.76	284.8	0.81	207.9	1.10	109.6	2.09	328.5	0.70	239.1	0.96	229.6	S
B6	232.9	1.13	228.8	1.15	686.8	0.38	481.7	0.55	507.5	0.52	304.5	0.86	263.2	F
B7	232.9	1.17	238.6	1.14	711.8	0.38	355.0	0.77	506.5	0.54	365.9	0.74	272.4	F
B8	443.0	0.50	406.0	0.55	285.7	0.78	136.6	1.63	273.0	0.82	183.0	1.22	223.2	B
B9	443.0	0.78	404.3	0.85	439.5	0.78	257.8	1.34	313.2	1.10	187.9	1.83	344.7	B

Failure forms: F is bending failure; B is bond splitting failure; S is shear failure, FB is bond splitting failure after bending failure, and FS is shear failure after bending failure.

6.2 Bending ultimate strength

Fig. 8 (a) shows the relationship of the maximum strength with the calculated value of the bending ultimate strength obtained by the equation in Ref. [1] for a total 6 specimens: P1 and B1 to B3 specimens with four SD600 longitudinal tensional rebars arranged in only the outside and B6 and B7 specimens with six SD600 longitudinal rebars arranged in the outside and the inside planned for bending failure.

In (b), the calculated value of the bending ultimate strength obtained by the equation in Ref. [2]. Q_e/Q_{fu1} is 1.01 to 1.22 times and Q_e/Q_{fu2} is 0.99 to 1.19 times.

Both equations were able to precisely evaluate the bending ultimate strength of beam members combining SD600 rebars with normal concrete.

6.3 Bond splitting strength, shear ultimate strength

Fig. 9 shows the relationships of maximum strength with the calculated values of bond splitting strength of 4 specimens: B4, B8, and B9 planned for bond splitting failure and P1 which ovserved bonding splitting failure after longitudinal rebar yeilding.

In Fig. 9 (a), Rp (Ref. [3]) is assummed to be 0. In (b), Rp (Ref. [3]) is assummed to be 0.02. Rp represents the factor of rotational angle level. Q_e/Q_{bu0} is 0.68 to 1.10 times and Q_e/Q_{bu2} is 1.04 to 1.83 times. Q_e/Q_{bu0} of B4 specimen with SD600-D19 longitudinal rebars arranged in only the outside was 0.92, confirming that it is possible to perform approximate evaluations with a current proposed equation.

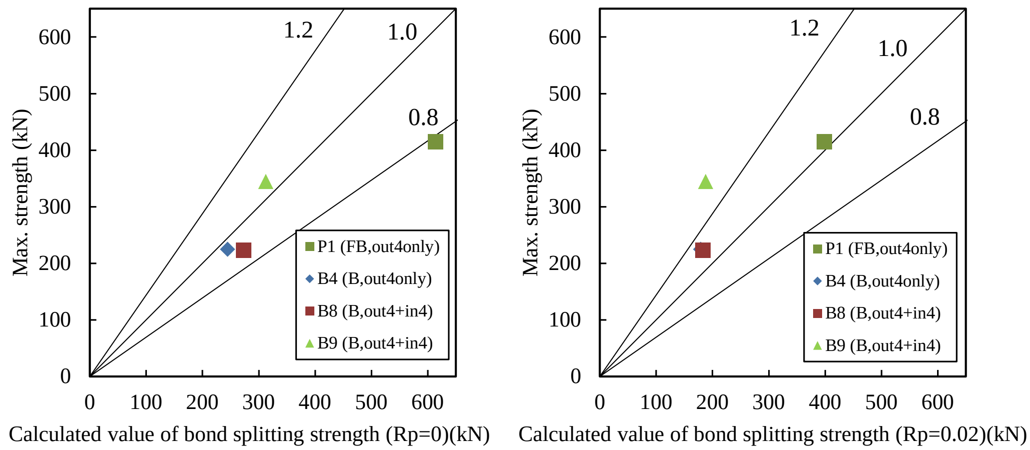

(a) Ref.[1] Equation (b) Ref.[2] Equation

Fig. 8 – Relationship of maximum strength with calculated value of bending ultimate strength

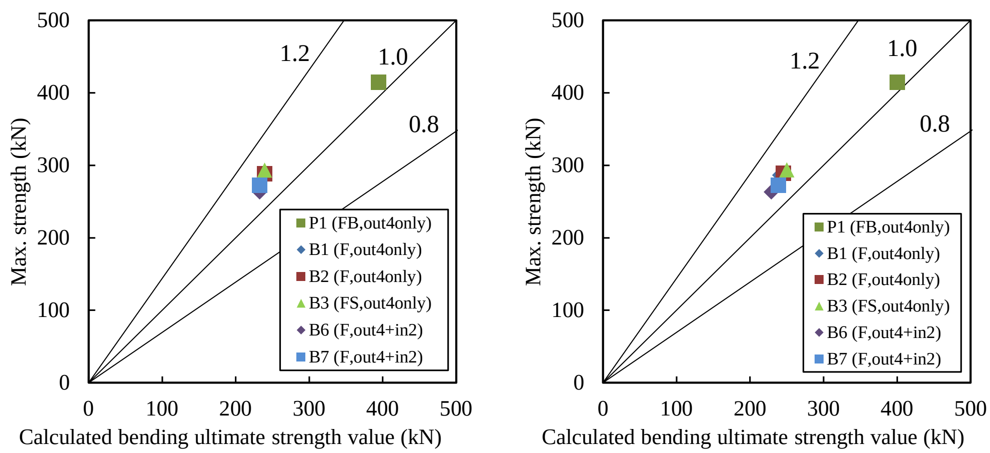

(a) Ref.[3] Equation (Rp=0) (b) Ref.[3] Equation (Rp=0.02)

Fig. 9 – Relationship of maximum strength with calculated value of bond splitting strength

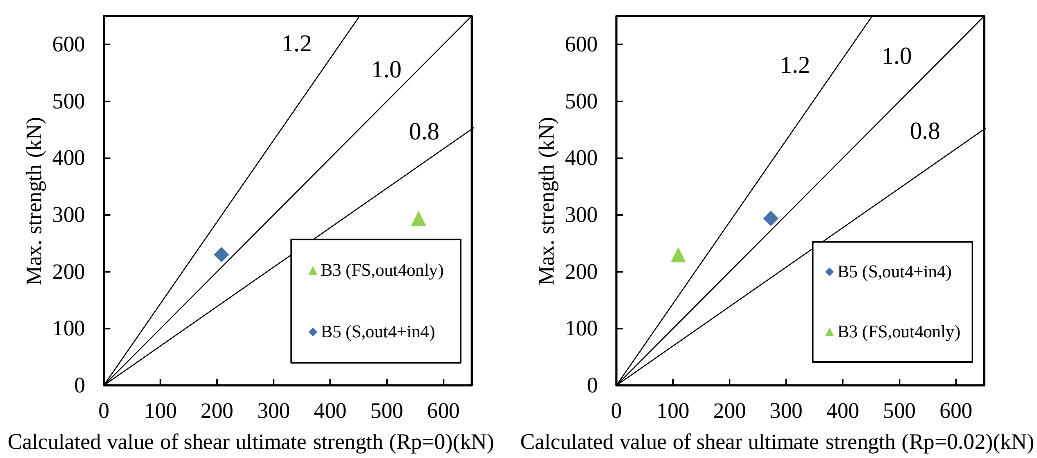

(a) Ref.[4] Equation (Rp=0) (b) Ref.[4] Equation (Rp=0.02)

Fig. 10 – Relationship of maximum strength with calculated value of shear ultimate strength

However, Q_e/Q_{bu0} of B8 specimen with SD600-D19 longitudinal rebars arranged in the outside and inside is 0.82. Because the rebar in the inside of the B8 specimen was not constrained by sub-ties, the maximum strength did not reach the calculated value. Hence, B9 the specimen is planned with sub-ties added to B8 specimen. Q_e/Q_{bu0} of B9 specimen was reached 1.10 times. Q_e/Q_{bu2} of P1 specimen was 1.04. From these discussions, it is possible to evaluate the bond slipping strength by the current proposed equation in Ref. [4].

Fig. 10 shows the relationship of the maximum strength and the calculated value of the shear ultimate strength of B5 specimen which planned shear failure and B3 which observed shear failure after longitudinal rebar yeilding. In Fig. 10 (a), Rp (Ref. [4]) is assummed to be 0. In (b), Rp (Ref. [4]) is 0.02. Q_e/Q_{su0} is 0.53 to 1.10 times and Q_e/Q_{su2} is 1.08 to 2.09 times. Thus, it can be roughly evaluated. Q_e/Q_{su2} of B3 specimen is 1.08. It is possible to evaluate the shear strength by the current proposed equation in Ref. [3].

6.4 Skeleton curves

Fig. 11 shows the comparison between test results and calculated trilinear skeleton curves of specimens P1, B1 to B3, B6, and B7 which underwent bending failure.

In Japanese structural design, trilinear models are usually made as a skeleton curve for seismic response. Fig.11 also includes the four stiffness decline rates (αy) in Ref. [5] and [6]. The initial stiffness was calculated based on Young's modulus of the beam materials. And the bending ultimate strength was calculated by Q_{fu2}. The yielded angle is calculated between the stiffness decline rate (αy) and bending ultimate strength.

Here, the evaluation equation Eq. (1) of Ref. [5] is called the Sugano Equation, and the evaluation equation Eq. (2) of Ref. [6] is called the Modified Sugano Equation.

Equation of stiffness decline rate (αy) in Ref. [5] (Sugano Equation)

$$\alpha y = (0.043 + 1.64 * n * pt + 0.043 * a/D)\,(d/D)^2 \quad \cdots\cdots\cdots \quad (1)$$

Equation of stiffness decline rate (αy) in Ref. [6] (Modified Sugano Equation)

$$\alpha y' = (0.043 + 1.64 * n * pt * (\gamma / \sigma y) + 0.043 * a/D)\,(d/D)^2 \quad \cdots\cdots\cdots \quad (2)$$

In all specimens, the stiffness decline rate (αy) at yield in the test, roughly correspond with calculations by Eq. (1). And the calculations by Eq. (2) are obtained by varying (γ) in Eq. (2) among 295, 345, and 390. The calculation by Eq. (2) with 295 as γ is lower than that with 390 as γ. All specimens with SD600 rebars are shown by this trend. However, the difference among 3 calculations of γ values is small. When γ is 295, the calculation by Eq. (2) is insignificantly smaller than the testing stiffness decline rate (αy) after yield.

From this discussion, Eq. (1) can roughly evaluate the test results, and Eq. (2) can accurately evaluate the test results.

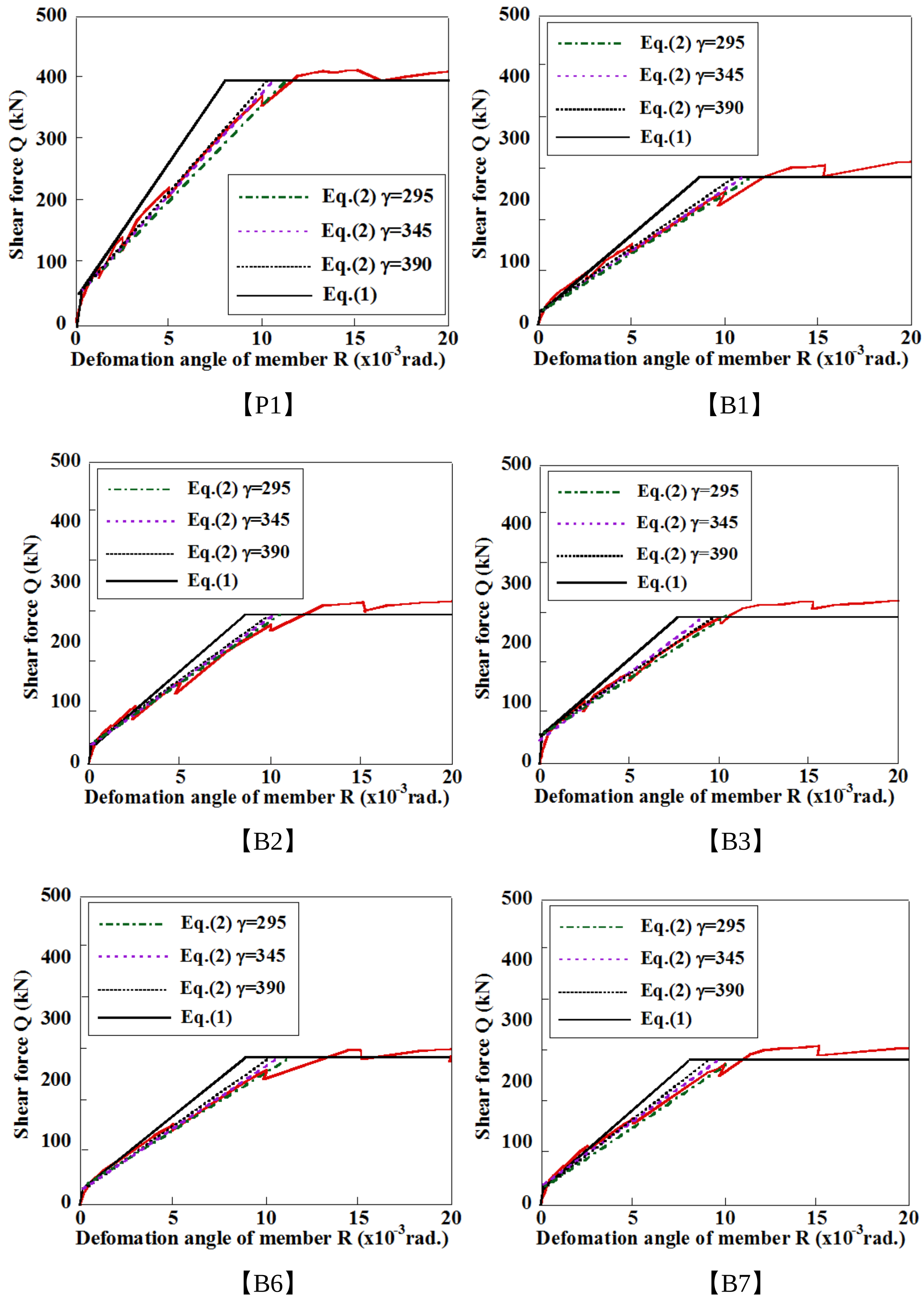

Fig. 11 – Comparison of the test and calculation of trilinear skeleton curves

7. Concluding Remarks

Thirteen RC beam specimens casted by combining longitudinal rebars with yield strength of 600N/mm^2 with concrete from 21 to 60N/mm^2 were tested. And investigations applying many calculation methods were carried out. The following knowledge was obtained.

1) The bending ultimate strength of a beam with longitudinal rebars with yield strength of 600N/mm^2 is accurately evaluated by AIJ formula (Ref. [1]) and ACI formula (Ref. [2]), regardless of the longitudinal rebar arrangement.

2) It is important to use sub-ties when two layers (outside and inside) of longitudinal rebars are set, in order to obtain substantial bond splitting strength.

3) Shear strength after longitudinal rebar yielding can be approximately evaluated by AIJ method with Rp=0.02 (Ref. [3]).

4) The comparison of the test and Sugano Equation for the skeleton curve shows taht the stiffness decline rate (αy) of the Sugano Equation is bigger than that in test result.

5) The Modified Sugano Equation with γ=295 to 390 as the stiffness decline rate (αy), can correspond with test result. The skeleton curves using the Modified Sugano Equation are available to design beams with 600N/mm^2 longitudinal rebars.

8. References

[1] Architectural Institute of Japan (2010). *AIJ Standard for Structural Calculation of Reinforced Concrete Structures Revised 2010*, (in Japanese).

[2] American Concrete Institute (2014). *Building Code and Commentary* ACI 318-14, USA.

[3] Architectural Institute of Japan (1990). *Design Guidelines for Earthquake Resistant Reinforced Concrete Buildings Based on Ultimate Strength Concept*, (in Japanese).

[4] Architectural Institute of Japan (1999). *Design Guidelines for Earthquake Resistant Reinforced Concrete Buildings Based on Inelastic Displacement Concept*, (in Japanese).

[5] Sugano Shunsuke (1973): Concrete Journal. *Research on restoring force properties of RC members*, Vol. 11, No. 2, 1 - 9, February, (in Japanese).

[6] Denno Satoshi et al. (2011): Concrete Engineering. *Experimental research on RC column-beam connections using super-strong materials*, Vol. 33, No. 2, 307 - 312, (in Japanese).